Thesis for Doctor of Philosophy

Criteria for selecting treatment according to cereblon protein expression in multiple myeloma

The Graduate School

of the University of Ulsan

Department of Medical science

Kim, yun kyu

Criteria for selecting treatment according to cereblon protein expression in multiple myeloma

Supervisor by Professor Shin Hwang

Submitted to
the Graduated School of the University of Ulsan
in Partial Fulfillment of the Requirements
for the Degree of

Thesis for Doctor of Philosophy

by

Kim, yun kyu

Department of Medical Science
Ulsan, Korea
February 2024

Criteria for selecting treatment according to cereblon protein expression in multiple myeloma

This certifies that the dissertation
Of Kim, yun kyu is approved

Dong Hwan Jung
Committee Vice-chair Dr.

Shin Hwang
Committee member Dr.

Gil Chun Park
Committee member Dr.

Gi Won Song
Committee member Dr.

Sun Hyung Joo
Committee member Dr.

Department of Medical Science

Ulsan, Korea

February 2024

Abstract

The treatment of Multiple Myeloma (MM) prioritizes combination therapy due to its effectiveness. Among of them, Immune-modulating drugs (IMiDs) commonly used as the anticancer agents for MM. The mechanism of action for IMiDs involves binding to the CRBN protein, a subunit of the E3 ubiquitin ligase complex by altering its substrate such as Ikaros (IKZF1) and Aiolos (IKZF3). These proteins leading to MM cell death or the regulation of the cell cycle and then inhibiting tumor growth.

To investigate the expression of CRBN protein, a monoclonal antibody that specifically binds to CRBN was produced using hybridoma cells, and the expression level of CRBN protein in various tissues was examined. As the results, the expression of CRBN protein was found in various tissues including heart, brain, lung, liver, skeletal muscle, kidney, and testis. Moreover, it was checked that the brain and immune like cell highly expressed CRBN protein.

To investigate the function of the CRBN protein in animal model, CRBN knock-out (KO) mice were generated and then the 2D gel electrophoresis was investigated to separate and analyze proteins with differential expression by using brain tissues from both normal and knockout mice. As the result, five proteins exhibiting differential expression were identified. Additionally, using these samples, the protein kinase assay was assayed to investigated the mechanism related to CRBN protein. As the previous reports, we confirmed that the CRBN protein is associated with the E3 ubiquitin ligase pathway.

We investigated that CRBN protein expression and cytotoxicity of IMDs in multiple myeloma cell lines. As the results, the CRBN expression rate was higher in the order of RPMI-8226, U226 H929, and also increased the cytotoxic efficacy of IMiDs. Additionally, we found that CRBN expression was higher HCC827 cells compared to HCC827/CLR cells, and the cytotoxic efficacy of IMiDs was also increased HCC827 cells compared to HCC827/CLR cells. Taken together, these results suggested that MMs and Lung cancers with highly CRBN expression were increased the cytotoxicity of IMiDs.

Expanding on previous findings that indicated an absence of cytotoxic efficacy of IMDs in rodents compared to humans, we created humanized CRBN knock-in (KI) mice with a two-amino acid modification. We also established an animal model of multiple myeloma using the mouse multiple myeloma cell line MOPC315-Luc (humanized CRBN). We transplanted the MOPC315-Luc cell line into CRBN KO and KI mouse models for multiple myeloma and treated them with IMD for 47 days. As a result, we observed a significant reduction in the size of multiple myeloma in humanized CRBN KI mice compared to CRBN KO mice. These results suggest that the degree of CRBN protein expression during treatment in MM influences the efficacy of IMiDs and that MM patients with high CRBN expression may benefit from treatment with a combination therapy containing IMiDs.

These data might be providing a basis for CRBN to be used as a novel target protein in MM to screen for therapeutics.

Keywords: Multiple myeloma, Cereblon, immunomodulatory drugs

Contents

List of Table and figures

ABBREVIATIONS

CRBN: Cereblon

ARNSMR: autosomal recessive non-syndromic mental retardation

CRL4: cullin 4-RING ubiquitin ligase

Roc1: RING finger protein

DDB1: DNA damage binding protein 1

BKCa: large conductance calcium-activated potassium channels

AMPK: adenosine monophosphate (AMP)-activated protein kinase

NF-kB: Nuclear factor kappa B

TLR: Toll-like receptors

BECN1: Beclin-1

TAB2: TGF-Beta Activated Kinase 1 (MAP3K7) Binding Protein 2

ECSIT: Evolutionarily conserved signaling intermediate in Toll pathways

TRAF6: Tumor necrosis factor receptor (TNFR)-associated factor 6

IL-1β: Interleukin 1 beta

IL-6: interleukin 6

COX-2: Cyclooxygenase 2

iNOS: Inducible nitric oxide synthase

LPS: lipopolysaccharide

Th17: T-helper 17

IL-2: Interleukin-2

IL-17A: Interleukin 17A

IFN-γ: Interferon Gamma

PERK: protein kinase R (PKR)-like endoplasmic reticulum kinase

eIF2α: eukaryotic translation initiation factor 2 alpha

Hsp70: heat shock protein 70

DNAJA1: DnaJ Heat Shock Protein Family (Hsp40) Member A1

ERK: Extracellular signal-regulated kinase

GSK3α/β: Glycogen synthase kinase 3α/β

ACC-α: Acetyl-CoA carboxylase 1

PPARα: Peroxisome proliferator–activated receptor α

PCK1: phosphoenolpyruvate carboxykinase 1

G6PC: glucose 6-phosphatase

BTG2: B-cell translocation gene 2

CREBH: cyclic AMP (cAMP)-responsive element-binding protein H

SESN2: sestrin2

SHP: small heterodimer partner

CYP2E1: Cytochrome P450 Family 2 Subfamily E Member 1

ROS: Reactive oxygen species

CB1R: cannabinoid receptor type 1

YY1: yin yang1

SIRT1: saltuin 1

MMP1: matrix metalloprotease 1

SCH: stratum corneum hydration

MEFs: mouse embryonic fibroblasts

IMiDs: immunomodulatory drugs

MM: multiple myeloma

KO: Knockout

KI: Knockin

Introduction

Cereblon is a protein encode by *CRBN* gene and is first discovered in the brains of patients with autosomal recessive non-syndromic mental retardation (ARNSMR) and is located 11 exons, 442 or 441 amino acids, and a molecular weight of 51 kDa.[1, 2] It is mainly found in the nucleus, cytoplasm, vesicles, peripheral membranes, and brain of various tissues.[3] and *CRBN* mRNA expression is found in various tissues such as the human brain, skeletal muscle, pancreas, liver, kidney, testis, and prostate.[Fig 1] Moreover, CRBN protein is also mainly expressed in Blood and Immune cells, brain, cardia, rectum, kidney, spleen, pancreas, placenta, ovary, etc.[Fig 2] It is well known that CRBN is the Cullin 4 ring E3 ligase complex (CRL4), which consists of Cullin 4, RING finger protein (Roc1), and DNA damage binding protein 1 (DDB1).[4] CRL4 is involved in DNA damage repair, regulating the cell cycle, and chromatin replication by targeting cellular substrates for ubiquitination.[5, 6] It was reported that CRBN regulate such as large conductance, calcium- and voltage-activated potassium (BKCa) channels, and CLC-1 chloride channels.[3, 7] Orai1, which maintains the balance of intracellular calcium levels, interacts with CRBN, is CRBN-dependent ubiquitinated and degraded, and is upregulated through weakened interaction with CRBN during efferocytosis, increasing calcium influx into phagocytes, and it promotes the removal of apoptotic cells by phagocytes.[8] With other functions, CRBN directly interacts with the α subunit of adenosine monophosphate (AMP)-activated protein kinase (AMPK α) and induces CRL4-CRBN-dependent degradation of the γ subunit, thereby inhibiting AMPK activation and regulating the signaling pathway.[3, 9, 10] Another efficacy of CRBN is receiving considerable attention due to its inflammation-modulating effect. In recent studies, CRBN is associated with autophagy and Nuclear factor kappa-light-chain-enhancer of activated B cells (NF-kB) activation induced by Toll-like receptor (TLR) 4 and inhibits ubiquitination of BECN1, TAB2, and ECSIT induced by TRAF6, thereby inhibiting autophagy, NF-kB activation, and bactericidal activity induced by TLR4.[11, 12] In addition, the reduction of c-Jun protein by CRBN is known to reduce AP-1 transcription activity and inhibit the expression of

inflammatory cytokines such as Interleukin 1 beta (IL-1β), interleukin 6 (IL-6), Cyclooxygenase 2 (COX-2), and Inducible nitric oxide synthase (iNOS) caused by lipopolysaccharide (LPS).[13] CRBN suppresses T-helper 17 (Th17) differentiation of $CD4^+$ T cells by suppressing the activity of $CD4^+$ T cells and secretion of Interleukin-2 (IL-2), and when CRBN is artificially removed from T cells, Interleukin 17A (IL-17A) and Interferon Gamma (IFN-γ) cytokines increase.[14] When *CRBN* was artificially deleted, AMPK showed high activity in various tissues and high protection against several diseases. In ischemic brain injury, the PKR-like endoplasmic reticulum (ER) kinase (PERK)/eukaryotic translation initiation factor 2 alpha (eIF2α) pathway is preactivated and resistant to various cell death stimuli, including ER stress.[15] Artificial removal of CRBN increases the Chaperone activity of heat shock protein 70 (Hsp70)/ DnaJ Heat Shock Protein Family (Hsp40) Member A1 (DNAJA1), reducing the phosphorylation and aggregation of Tau, increasing Tau's affinity for microtubules, reducing the accumulation of tau throughout the brain and reducing the activity of tau-kinases including p38, Extracellular signal-regulated kinase (ERK) and Glycogen synthase kinase 3α/β (GSK3α/β) to regulate the protein toxicity of Tau.[16] In ischemic heart injury, CRBN prevents damage caused by ischemia–reperfusion (I-R) by regulating AMPK activity.[17] In addition, CRBN selectively degrades $Ca_v1.2α$, leading to cardiac dysfunction.[18] In obesity caused by a high-fat diet, AMPK-α activation and Acetyl-CoA carboxylase 1 (ACC-α) inhibition showed a protective effect against obesity, fatty liver, and insulin resistance.[19] In alcohol-induced fatty liver disease, activation of Peroxisome proliferator–activated receptor α (PPARα) prevents alcohol-induced fatty liver disease and inflammation by reducing the inhibition of AMPK by CRBN.[20] Increased hepatic gluconeogenesis due to fasting and diabetes conditions results in increased phosphoenolpyruvate carboxykinase 1 (PCK1) / glucose 6-phosphatase (G6PC) expression by upregulation of the CRBN - B-cell translocation gene 2(BTG2)- cyclic AMP(cAMP)-responsive element-binding protein H(CREBH) signaling pathway, and increased sestrin2(SESN2) and small heterodimer partner (SHP) induced by melatonin inhibits the CRBN-BTG2-CREBH signaling pathway, inhibiting hepatic gluconeogenesis.[21] Alcohol significantly increases Cytochrome P450 Family 2 Subfamily E Member 1 (CYP2E1) enzyme

activity and Reactive oxygen species (ROS) production through the cannabinoid receptor type 1 (CB1R)-CRBN-yin yang1 (YY1) signaling pathway, causing liver damage by alcohol, and saltuin 1 (SIRT1) upregulation by melatonin inhibits the CB1R-CRBN-YY1 signaling pathway to protect liver damage.[22] In sepsis, CRBN regulates AMPK and heme oxygenase 1 to protect against the risk of immune response and organ failure.[23] In addition, streptozotocin-induced diabetic osteoporosis in mice with artificial deletion of CRBN is resistant to increased AMPK-α/ACC-α activation and inhibition of the IκBα/NF-κB pathway.[24] CRBN-Knockout (KO) mouse, protein levels of matrix metalloprotease 1 (MMP1) was increased but stratum corneum hydration (SCH) and collagen I expression were decreased. Additionally, mouse embryonic fibroblasts (MEFs) showed G2/M cell cycle arrest through upregulation of p21 by activation of p38 MAPK/p53.[25] These results indicated that involved in diverse functions and metabolism, has been proven to be a direct binding target, and has shown various effects upon direct binding to immunomodulatory drugs (IMiDs), especially Thalidomide. It has been extensively studied in pharmaceutical, clinical, and cancer fields, especially multiple myeloma(MM).[26]

Thalidomide's Molecular Formula is C13H10N2O4 and contains a glutarimide ring and a variable phthaloyl ring.[27] Thalidomide was first known in the 1950s as a preventive agent for morning sickness in pregnant women, but was withdrawn in the 1960s due to serious side effects that led to limb deformities in the fetus.[28, 29] Thalidomide was used as a short-term treatment for Erythema Nodosum Leprosum in 1965 and has since been studied for treatment applications for other diseases.[30, 31] After its withdrawal, it was discovered to be effective in immune regulation, anti-inflammation, and anti-cancer, and was actively studied again.[32] CRBN directly interacts with thalidomide and inhibits its ubiquitin ligase activity, causing malformations.[33] In 1994, Thalidomide was shown to inhibit fibroblast growth factor (bFGF)-induced angiogenesis.[34] Thalidomide is effective in the treatment of inflammatory bowel disease and rheumatic diseases, as well as its anticancer effect on MM.[35-37] Thalidomide has been reported to be clinically effective against MM and myelodysplasia.[38, 39] In a recent study, Thalidomide regulates the immune response by regulating the IFN-γ, Tumor necrosis factor (TNF)-α, COX-

2, IL-6, IL-10, IL-12, and NF-κB.[40-45] Immunomodulatory properties are mediated by antifibrotic effects by inhibition of fibroblast growth factor and anti-inflammatory activity through TNF-α blocking.[46-48] angiogenesis plays an important role in MM.[49, 50] thalidomide was first used in relapsed/refractory MM in 1998.[51] thalidomide/lenalidomide were each approved as a treatment for multiple myeloma in 2006.[52] IMiDs, such as thalidomide, lenalidomide, and pomalidomide, is used in the treatment of MM, deletion (5q) myelodysplastic syndrome (del(5q) MDS), chronic lymphocytic lymphoma (CLL), and many patients with multiple myeloma have substantially improved survival rates in modern combination therapy, including immunomodulators (lenalidomide and lenalidomide) and proteasome inhibitors, but treatment success rates are still low.[53] The immunomodulatory and anti-proliferative effects of IMiDs are related to the degradation and ubiquitination of Ikaros (IKZF1) and Aiolos (IKZF3) transcription factors by the CUL4-RBX1-DDB1-CRBN (CRL4CRBN) E3-ligase complex.[54-57] Additionally, the level of CRBN can be said to be an important factor in determining the effectiveness of drug treatment in myeloma cells.[58] Although IMiDs and CUL4-RBX1-DDB1-CRBN (CRL4CRBN) E3-ligase complex combination have affect MM, the selection of appropriate IMiDs according to CRBN level is unclear. Therefore, this study investigated the relationship between CRBN level and IMiDs for dramatic therapeutic effects in multiple myeloma treatment.

Multiple myeloma occurs mainly in patients over 65 years of age, also known as geriatric blood cancer, and the number of patients with Multiple myeloma is increasing rapidly. Multiple myeloma treatments have been developed to help patients, but the problem is that despite these treatments, the disease progresses quickly and has a high chance of recurrence. In the latest treatment guidelines of the National Comprehensive Cancer Network (NCCN), anti-cancer combination therapy (carfilzomib and dexamethasone alone (Kd), carfilzomib and lenalidomide plus dexamethasone (KRd), elotuzumab and lenalidomide plus dexamethasone (ERd), ixazomib and lenalidomide plus dexamethasone (IRd), daratumumab and botezomib plus dexamethasone (DVd), Daratumab and lenalidomide plus dexamethasone (DRd) is the top recommendation. Despite treatment based on the top recommendation, anti-cancer drugs are randomly selected and used due to a lack of research on

treatment mechanisms. Therefore, new targeted and optimal combination therapy is needed through various studies of Multiple myeloma mechanisms. The aim of this study was to clarify the direct relationship and mechanism of CRBN and IMiDs in Multiple myelomas and to establish criteria for selecting selective treatments according to CRBN protein expression.

Materials and methods

Cells, Antibodies, and Reagents

Cells, including U226, RPMI-826, H929, MOPC315, H1975, H820, A549, H460, H1573, H2009, LK-2, Calu-1, H1299, H3122, H228, HCC366, H2286, H1581, H520 PC-9, HCC827, and PC-9 mutations, HCC827 mutations, were cultured in RPMI-1640 Medium and DMEM Medium supplemented with 10% fetal bovine serum, penicillin, and 100 μg/ml streptomycin (Gibco BRL Gaithersburg, MD). Antibodies specific to AMPK, DDB1, Cul4 were procured from Cell Signaling Technology (Beverly, MA), while HA tag, Anti-α-Tubulin antibody, and anti-β-actin antibody were sourced from Santa Cruz Biotechnology (Santa Cruz, CA). The enhanced chemiluminescence western blotting detection reagent was obtained from Amersham (Buckinghamshire, UK). Carfilzomib, Elotuzumab, Ixazomib, and Daratumumab were purchased from Sigma-Aldrich (St. Louis, MO). Thalidomide, Lenalidomide, Pomalidomide, and MTT (3-[4,5-dimethylthiazol-2-yl]-2,5-diphenyltetrazolium bromide), along with other chemicals, were also procured from Sigma-Aldrich (St. Louis, MO).

Cell culture

Cell lines (U226, RPMI-826, H929, MOPC315, H1975, H820, A549, H460, H1573, H2009, LK-2, Calu-1, H1299, H3122, H228, HCC366, H2286, H1581, H520, PC-9, HCC827, and PC-9 mutation, HCC827 mutation) were procured from the Korean Cell Line Bank (KCLB). Cultures were maintained in an incubator at 37°C with an atmosphere containing 5% CO2, while the cells were cultured in RPMI and DMEM media supplemented with 5% fetal bovine serum (FBS) and 1% anti-anti.

Cell treatment and Cell viability assay

Dimethyl sulfoxide (DMSO) was used to dissolve Thalidomide, Lenalidomide, and Pomalidomide, which were then directly added to the culture media. For cell

viability assessment, cells were seeded at a density of 3x10^4 cells/well in 48-well plates with an overnight incubation. Following 24 hours, the cells were subjected to treatment with Thalidomide, Lenalidomide, and Pomalidomide at concentrations ranging from 0 to 100 µg/ml. After a 24-hour incubation period, 100 µl of MTT solution (1mg/ml) was added to each well, and the cells were incubated for 2 hours at 37°C in a humidified atmosphere with 5% CO2. Subsequently, the culture medium was removed, and 100 µl of DMSO was added to each well for 1 minute at room temperature. The absorbance at 595 nm was measured using an ELISA reader (PerkinElmer, USA), with this wavelength chosen to avoid interference with IMiDs.

shRNA Lentiviral Transduction

CRBN shRNAs and scrambled shRNA were acquired from Santa Cruz Biotechnology (Santa Cruz, CA). Following the manufacturer's protocol, MOPC315 cells were transfected with shRNA using the Transduction reagent, Hexadimethrine Bromide, and Puromycin (Sigma-Aldrich St. Louis, MO). For each construct, 1.6 x 10^4 cells were seeded in fresh media into the required number of wells in a 96-well plate. Duplicate or triplicate wells were utilized for each lentiviral construct and control. Incubation was carried out for 18-20 hours at 37°C in a humidified incubator with an atmosphere of 5-7% CO2. The next day, media were removed from the wells. Subsequently, 110 µl of media and Hexadimethrine bromide (final concentration 8 µg/ml) were added to each well, and the plate was gently swirled for mixing. After 24 hours, the media containing lentiviral particles were removed. Fresh media (120 µl) were added to each well 24 hours later, followed by the removal of media from the wells. Finally, fresh media containing puromycin were added, and the media with fresh puromycin were replaced every 3-4 days.

Transient transfection and luciferase assay

Overnight, cells (3 × 10^5 cells/well) were replated in 24-well plates and subjected to transient co-transfection with the MOPC315-promoter-luciferase construct and pRL-SV plasmid (Promega, USA). LipofectAMINE ™ 2000 reagent (Invitrogen,

USA) was utilized for the transfection process. The calculation of relative luciferase activities involved normalizing MOPC315-promoter-driven firefly luciferase activity to Renilla luciferase activity.

Production of monoclonal antibodies against CRBN

To produce a monoclonal antibody against cereblon (CRBN), suitable antigen peptide sequences were selected based on hydrophilicity and hydrophobicity measurements from the CRBN sequence. The peptides C-EDEMEVEDQDSKEAK (28-42aa, 16mer), C-DMEEFHGRTLHD (63-74aa, 13mer), C-EIYAYREEQDFGIE (140-154Aa, 15mer), C-GRQRFKVLELRTQSD (161-175aa, 16mer), and C-DRIKKQLREWDENLKD (255-270aa, 17mer) were conjugated to keyhole limpet hemocyanin (KLH) and Bandeiraea simplicifolia agglutinin (BSA) using SuccinIMiDsyl 4-(N-maleIMiDsomethyl) cyclohexane-1-carboxylate (SMCC) and screened via ELISA for antigen production. Recombinant CRBN proteins PEP2, PEP4, and PEP5 (each at 30 μg/μL) were mixed, diluted in phosphate-buffered saline (PBS) to 150 μL, and emulsified with an equal volume of complete Freund's adjuvant. This emulsion was injected into the peritoneal cavity of BALB/C mice every three weeks for a total of four injections. One month after the fourth immunization, spleens were harvested from the mice that received purified CRBN protein via tail vein injection. Hybridoma cells were generated by fusing spleen cells with myeloma cells, and specific hybridoma clones reacting only to CRBN were screened using enzyme-linked immunosorbent assay (ELISA). Selected hybridoma cell lines ("1D3" and "4E11") were used to produce monoclonal antibodies against CRBN. Female Balb/C mice (7-8 weeks old) were injected with 500 μL of pristane into the abdominal cavity. After 7-10 days, hybridoma cells [1D3 and 4E11] selected from a 75T/C culture flask were injected into the peritoneal cavity of mice ($8x10^5$ to $4x10^7$ cells per mouse). Ascites fluid was collected 5-7 days later using an 18G needle. The collected ascites fluid was kept at 4°C overnight, centrifuged the next day to remove debris, and the supernatant was separated. The separated supernatant was stored at -20°C. After filling an appropriate column with the stored supernatant, 20% ethanol was used to wash, followed by elution with 3 bed volumes of binding

buffer (20 mM sodium phosphate, pH 7.0) and 3 bed volumes of elution buffer (0.1 M glycine buffer, pH 3.0-2.5) in 0.5 mL fractions. Each fraction was neutralized with 35 µL of neutralization buffer (1 M Tris-HCl, pH 9.0). The eluted fractions were ethanol-precipitated at 70% ethanol, stored in 20% ethanol until the next use, and purified using desalting columns (Ammersham GE). The purity of each fraction was confirmed by SDS-PAGE, and the monoclonal antibody against CRBN was purified.

Immunoprecipitation (IP)

An anti-HA immunoprecipitation kit from Sigma-Aldrich (St. Louis, MO) was employed to perform HA-immunoprecipitation in accordance with the manufacturer's instructions. A cellular homogenate was prepared by lysing cells in 600 µl of lysis buffer (containing 50 mM Tris-HCl, pH 7.5, 150 mM NaCl, 1% Nonidet P40, 0.5% sodium deoxycholate, 1 X protein inhibitor cocktail from Sigma-Aldrich St. Louis, MO, and 5 mM DTT) and subsequently centrifuged for 10 minutes at 12,000 x g at 4°C. The resulting supernatant was then mixed with 15µl of anti-HA agarose beads suspension and allowed to incubate for 3 hours at 4°C. Following incubation, the agarose beads underwent a series of washes: four times with 1x IP buffer and an additional wash with 0.1x IP buffer. The thoroughly washed agarose beads were resuspended in 30 µL of loading buffer and subjected to heating at 95°C for 5 minutes. Subsequent removal of beads was achieved through centrifugation, and the resulting flow-through was subjected to analysis by SDS-PAGE.

2d gel electrophoresis

The protein solution was rehydrated with Immobilin DryStrip pH 3-10NL, 24 cm (Amersham Biosciences, UK), at the strip anchor for 16 hours at room temperature. One-dimensional isoelectric focusing (IEF) was performed using the Multiphor electrophoresis system (Amersham Biosciences, UK). Electrophoresis was conducted at a temperature of 20°C with the following protocol: Step 1: 100 V for 4 hours, Step 2: 300 V for 2 hours, Step 3: 600 V for 1 hour, Step 4: 1000 V for 1 hour, Step 5: 2000 V for 1 hour, Step 6: 3500 V for 27 hours. After IEF, fixed pH gradient

(IPG) strips underwent alkylation through the first step reduction by TBP equilibrium buffers (6M Urea, 2% SDS, 30mM Tris, 20% glycerol, 2.5% acrylamide solution, and 5mM TBP) for 25 minutes. Subsequently, the strips were subjected to two-dimensional 9% to 16% SDS-PAGE using the Ethan Daltwellve (Amersham Biosciences, UK) electric mobility system. The electric transfer temperature was set to 20°C, with the first stage at 2.5W/gel for 30 minutes and the second stage at 16W/gel for 6 hours. For gel preparation in IEF/SDS-PAGE, 1 mg of internal standard protein was used, and visualization of the gel was achieved with either Coomassie Blue R-250 or silver dye (Sigma-Aldrich St. Louis, MO).

Western blotting

Protein samples underwent a 5-minute heating at 95°C, followed by analysis using sodium dodecyl sulfate polyacrylamide gel electrophoresis (SDS-PAGE) and subsequent electrophoretic transfer to an Immune-Blot™ polyvinylidene difluoride (PVDF) membrane (Bio-Rad Laboratories). Primary rabbit antibodies, including anti-CRBN and anti-β-actin antibodies, were used to incubate the membranes. Immunoblot signals were developed using enhanced chemiluminescence (Pierce Biotechnology, Rockford, IL), and analysis was performed with the ImageQuant™ LAS 4000 biomolecular imager (GE Healthcare Life Sciences, Waukesha, WI) and bundled Multi Gauge 3.0 software. The values presented in the western blot figures denote the relative density of the bands normalized to that of β-actin.

ELISA

ELISA kits (Sigma-Aldrich St. Louis, MO) were employed to quantify IgM levels in the culture medium following the manufacturer's instructions. In summary, polyclonal goat anti-mouse cytokine antibodies served as primary antibodies, and detection was facilitated using biotinylated polyclonal goat anti-mouse antibodies. Each assay involved generating a standard curve, and colorimetric changes were measured at 450 nm.

Generation of CRBN KO mice

To generate CRBN knockout (KO) mice, the knockout mouse service (Macrogen, Seoul, Korea) provided heterozygous F1 animals. A targeting vector, designed to delete a segment encompassing exon 1 of the CRBN gene (1.1 kb), was constructed using a 5′ short arm fragment (2.6 kb) and a 3′ long arm fragment (7.3 kb), which were ligated into the pOsdupdel vector. The 1.1-kb genomic segment was replaced with the neomycin cassette in the targeting vector. Heterozygous F1 animals were subjected to over 10 generations of backcrossing with C57BL/6N mice before this study. Subsequent breeding of heterozygous males and females resulted in the production of CRBN KO mice. Genotypes of the wild-type (WT) and CRBN KO mice were determined by reverse transcription-polymerase chain reaction (RT-PCR) using tail genomic DNA and primers specific for WT or CRBN KO alleles.

Generation of CRBN KI mice

To generate CRBN knock-in (KI) mice, heterozygous F1 animals were provided by the knockin mouse service (Asan Medical Center, Seoul, Korea). Amino acid 380 V in the Balb/c mouse was mutated to E, and 391 I was mutated to V. Heterozygous F1 animals underwent backcrossing with Balb/c mice for a minimum of 10 generations before commencement of this study. Subsequent breeding of heterozygous males and females led to the production of CRBN KI mice. Genotypes of the wild-type (WT), CRBN knockout (KO), and CRBN KI mice were determined by reverse transcription-polymerase chain reaction (RT-PCR) using tail genomic DNA and primers specific for WT, CRBN KO, or CRBN KI alleles.

Animals Care

CRBN knockout (KO) mice (male, Balb/c backcrossed to C57BL/6, 8-weeks old) and wild-type (WT) Balb/c mice were purchased from Koatech Laboratory Animal Company (Pyeongtaek, Korea). Maintained under standard laboratory conditions, the animals had access to free standard rodent food and water, following a 12-hour

light/dark cycle, with temperatures set at 21–24 °C and relative humidity at 40–60%. All animals were raised under specific pathogen-free conditions, and the experimental protocol was reviewed and approved (2022-12-074) by the Animal Subjects Committee of Asan Medical Center (Seoul, Republic of Korea).

Immunohistochemical (IHC) staining

Following sacrifice, the mice's tumors underwent fixation with 10% neutral buffered formalin, followed by paraffin embedding and slicing into 4 μm thick sections using a microtome. The sections were then subjected to 2 hours of heating at 60°C in a drying oven. The immunohistochemical examination of CRBN expressions in replicate sections of tissue-microarrayed slides was conducted using a mouse anti-CRBN antibody. In brief, antigen retrieval was performed, and endogenous peroxidase activity was quenched with hydrogen peroxide. Blocking serum provided in the staining kit was used to block the slides. Subsequently, the slides were incubated with the primary anti-CRBN antibody (1:100), followed by incubation with post-primary blocker and polymer, according to the manufacturer's instructions. Chromogen 3,3'-diaminobenzidine was utilized, and the slides were observed under a Digital microscope Coolscope II (Nikon, Japan).

Cancer cell transplantation

Mice of both female and male Balb/c, CRBN knockout (KO), and CRBN knock-in (KI) strains, aged six to eight weeks, were housed in pathogen-free conditions at room temperature for cancer cell transplantation. Subcutaneous injection of cells ($1x10^6$) in Matrigel (Corning, USA) into the right flanks of the mice was performed. Treatment initiation occurred when xenografts reached volumes of approximately 50 mm^3. Mice received daily intraperitoneal injections of 100 μl PBS as a control vehicle or IMiDs (0~1000uM). Tumor volume was recorded daily, and tumor length (L) and width (W) were measured using a Vernier caliper. Tumor volume was

calculated using the formula: Tumor volume (mm^3) = ½ x (tumor length) x (tumor width)^2. At the experiment's endpoint, tumors were removed and weighed. Sacrifices were carried out under CO2, with efforts made to minimize animal suffering. Portions of xenograft tissues were preserved in 10% Neutral Buffered Formalin and embedded in paraffin for pathological assessment, while the remaining tissues were processed for protein extraction and stored at -20˚C.

Statistical analysis

Experiments were replicated a minimum of three times, and the results are presented as the mean±standard deviation. Data analysis involved employing one-way ANOVA followed by Student's t-test to identify significant differences. The Kaplan-Meier method was utilized for comparing mortality rates between groups, and statistical significance was determined with p-values <0.05 and p-values <0.01 considered as statistically significant.

Results

Activity of the produced CRBN monoclonal antibody

The production of monoclonal antibodies against CRBN was successfully achieved using hybridoma cells generated from five peptide sequences with a high likelihood of monoclonal antibody production. (Fig 3A) The functionality and specificity of these antibodies were confirmed through Western blot analysis, demonstrating their precise and effective performance. Additionally, immunostaining with tissues further validated the accurate functionality of the antibodies. (Fig. 3B)

Expression of CRBN in various tissues

To validate the bioinformatics results, we utilized the newly developed monoclonal antibody to measure the levels of CRBN protein in various tissues of mice. The investigation into CRBN protein expression levels revealed its presence in diverse tissues, including the brain, heart, liver, lungs, skeletal muscles, kidneys, and testes. Notably, the highest expression was observed in the brain and immune cells, as confirmed by Western blot analysis. (Fig. 4)

Purified CRBN contains various proteins.

To identify protein differences between CRBN knockout (KO) and wild-type (WT) brains, we conducted 2D electrophoresis and identified six proteins that exhibited differential expression. (Fig. 5A) Through bioinformatics analysis, we confirmed that these six proteins interact with CRBN, highlighting their potential association with CRBN function in brain tissues. (Fig. 5B)

Effect of IMiDs on the level of CRBN protein

To investigate the effect of IMiDs according to CRBN protein expression, Western blot and cell viability were measured in various multiple myeloma cells. Among the multiple myeloma cell lines, H929 cells had the highest CRBN level, followed by U226 cells, RPMI-8226 cells were the lowest, and were confirmed using the western.

(Fig. 6A) When IMIDS was treated on multiple myeloma cell lines, the effect of IMIDS was highest at high CRBN levels depending on the CRBN level, (Fig. 6D) the effect was not good when the CRBN level was lowest, (Fig. 6C) and the effect was better than the lowest CRBN level at the medium CRBN level. (Fig. 6B)

Protein kinase associated with CRBN

To investigate proteins interacting with CRBN, a Protein Kinase Assay was conducted. (Fig. 7A) The results indicated involvement in transcription processes, particularly with CDK7 and CDK8, as well as participation in proto-oncogenes, specifically with PIK3 and MAPK kinases. (Fig. 7B)

The efficacy of IMiDs in cancer types other than multiple myeloma.

To investigate cancers other than liver cancer, the expression levels of CRBN protein were measured using Western blot in lung cancer cell lines. (Fig. 8A) Upon treatment with the IMiDs thalidomide, similar to multiple myeloma, a higher expression of CRBN correlated with better efficacy of IMiDs. (Fig. 8B) This suggests that, even in lung cancer, beyond multiple myeloma, one can anticipate the therapeutic effects of IMiDs based on the expression of CRBN.

Generation of CRBN KO mice and humanized CRBN.

To generate CRBN knockout (KO) mice, heterozygous F1 animals were supplied by the knockout mouse service (Macrogen, Seoul, Korea). The knockout strategy involved utilizing a targeting vector to delete a segment encompassing exon 1 of the CRBN gene (1.1 kb). This vector was constructed by ligating a 5′ short arm fragment (2.6 kb) and a 3′ long arm fragment (7.3 kb) into the pOsdupdel vector. The 1.1-kb genomic segment was replaced with a neomycin cassette in the targeting vector. Following at least 10 generations of backcrossing with C57BL/6N mice, heterozygous F1 animals were utilized to breed CRBN KO mice. Genotyping of WT and CRBN KO mice was performed using RT-PCR with tail genomic DNA and primers specific for wild-type (WT) or CRBN KO alleles (P1, P2, and P3 in Fig.

9A). To humanize mouse CRBN, amino acid 380 V was mutated into E and 391 I into V. (Fig. 9B) The anticancer effect of IMiDs (Lenalidomide) increased when CRBN was removed and humanized CRBN was transmitted to MOPC315 cells. (Fig. 9C)

Efficacy of IMiDs in CRBN KO and KI mice.

A multiple myeloma model was created by injecting MOPC 315-Luc cells into CRBN KO and KI mice. Tumors reached a size of about 50 mm3, mice were randomly divided into two groups: control (PBS) vs. IMiDs (10mg/kg). When IMiDs were treated three times for 47 days, compared to the control group, the KO group showed a slight decrease in tumor size, and the KI group showed a significant decrease in tumor size compared to the KO group. (Fig. 10)

Effectiveness of anti-cancer drugs according to CRBN level using multiple myeloma animal models.

A multiple myeloma model was created by injecting MM cells into (CRBN KO or KI mice. Tumors reached a size of about 50 mm3, mice were randomly divided into two groups: control (PBS) vs. anti-cancer drugs (10mg/kg). Multiple myeloma models showed various therapeutic effects according to the type of anti-cancer drugs. (Fig. 11A) Immunostaining of tumors showed more dramatic therapeutic effects at lower CRBN levels and higher levels (Figure 11C) (Figure 11B).

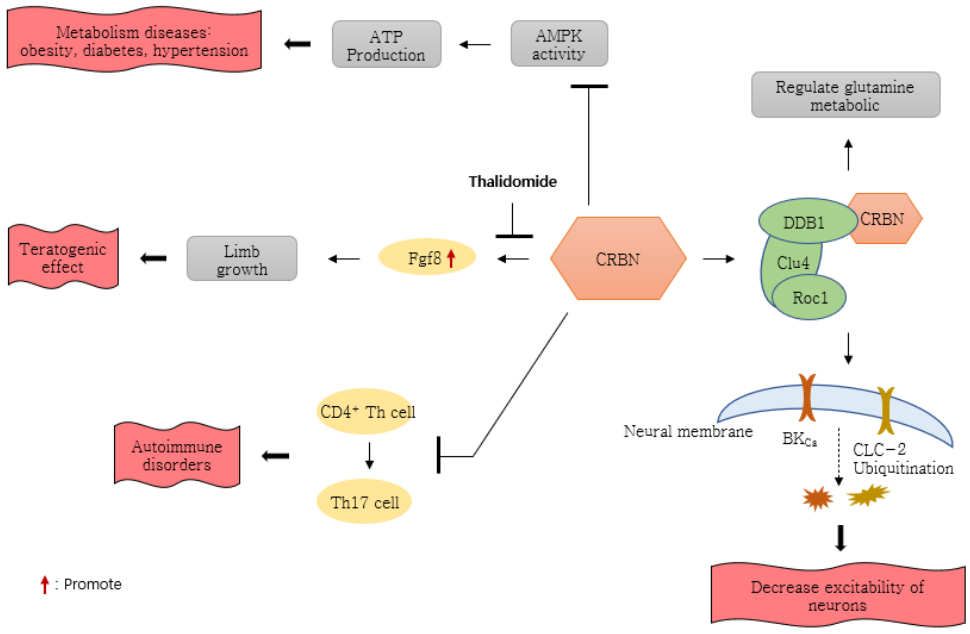

Diagram 1. Different roles of CRBN.

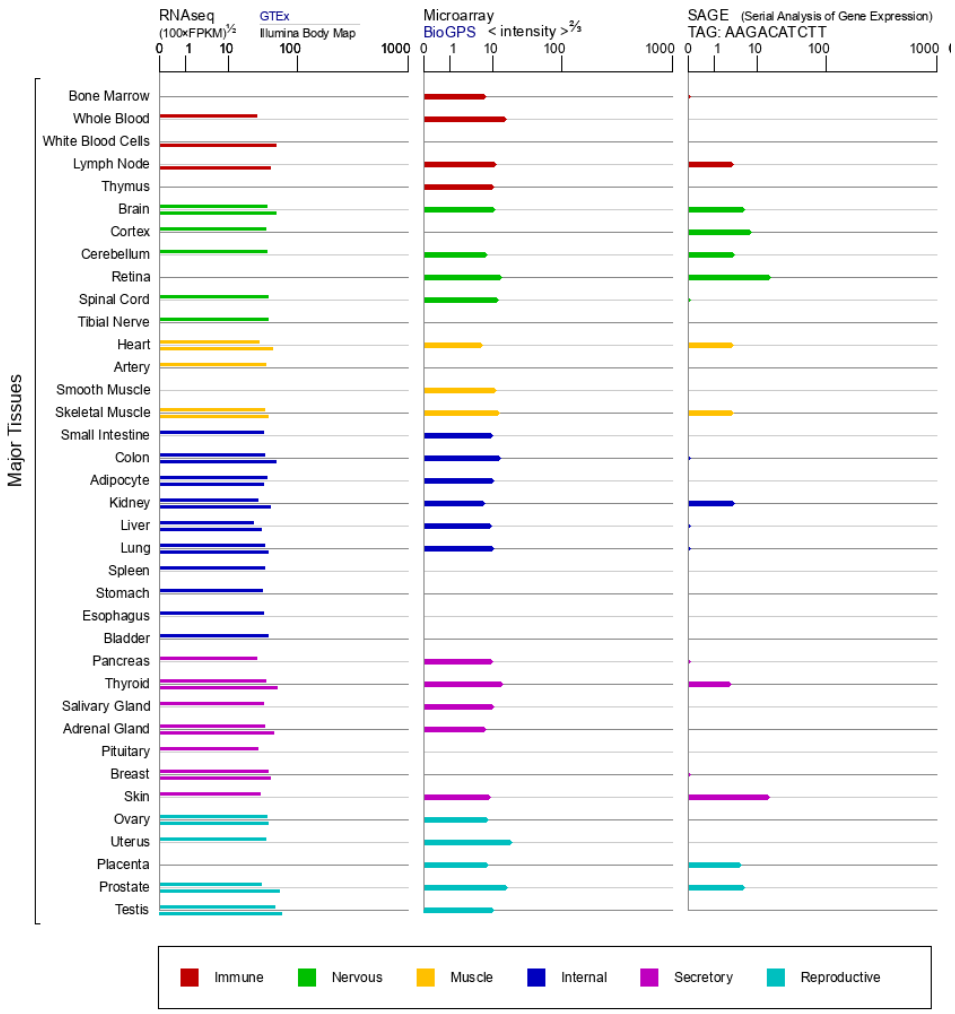

Figure 1. mRNA expression in normal human tissues from GTEx, Illumina, BioGPS, and SAGE for CRBN Gene.

(https://www.genecards.org/cgi-bin/carddisp.pl?gene=CRBN)

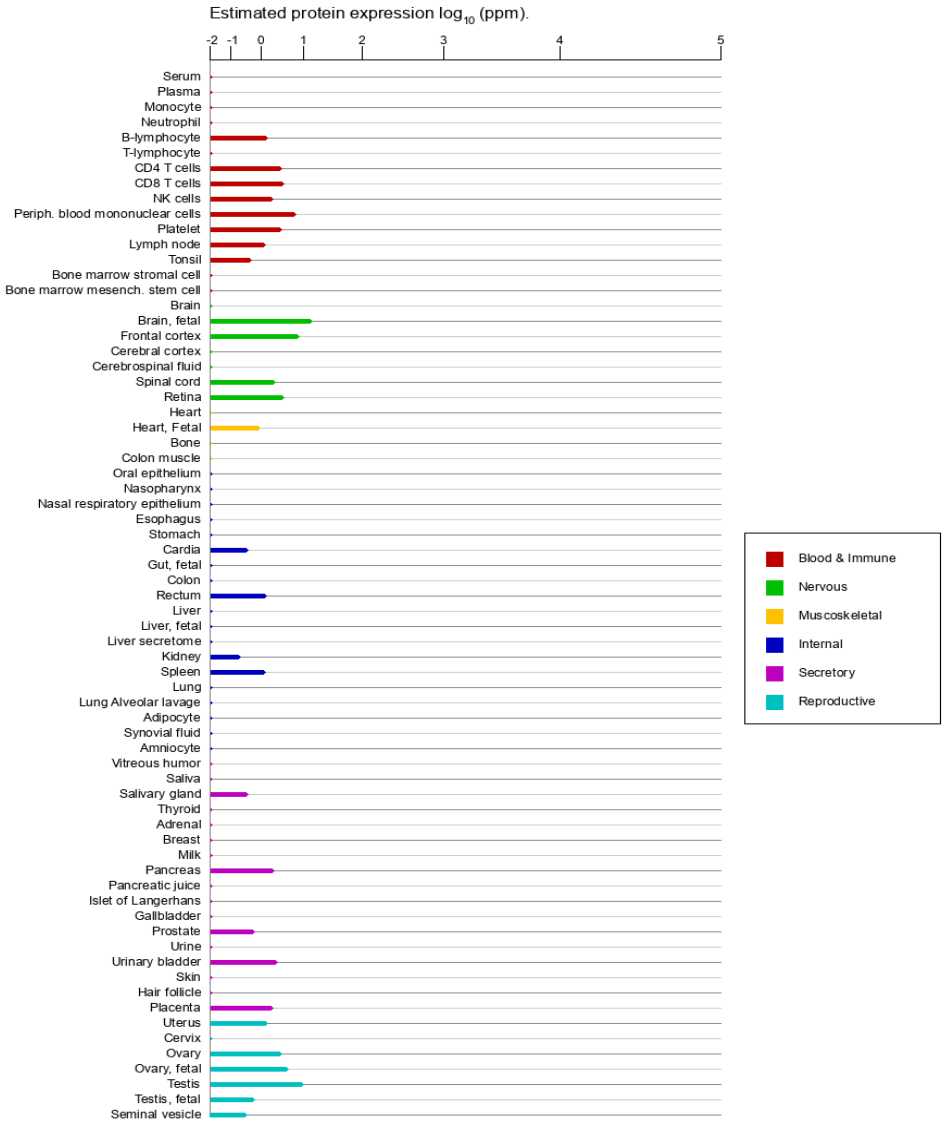

Figure 2. protein expression in normal tissues and cell lines from ProteomicsDB, MaxQB, and MOPED for CRBN Gene.

(https://www.genecards.org/cgi-bin/carddisp.pl?gene=CRBN)

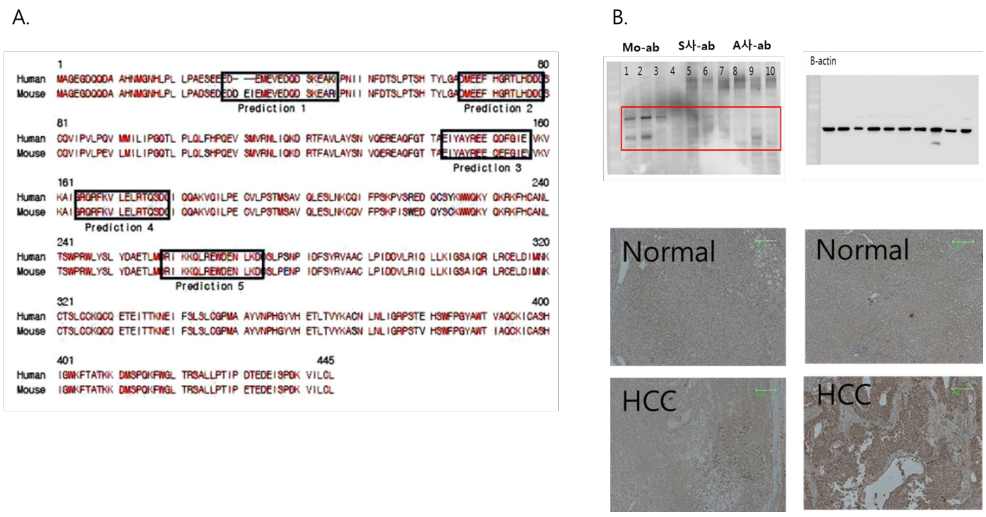

Figure 3. Activity of the produced CRBN monoclonal antibody.

To produce the CRBN antigen, we selected five peptide sequences from the CRBN sequence with a high potential for generating monoclonal antibodies. Using these five peptide sequences(a), we generated CRBN monoclonal antibodies with hybridoma cells, and their precise functionality was confirmed through Western blot analysis. Additionally, immunostaining with tissues also demonstrated accurate performance of the antibodies(b).

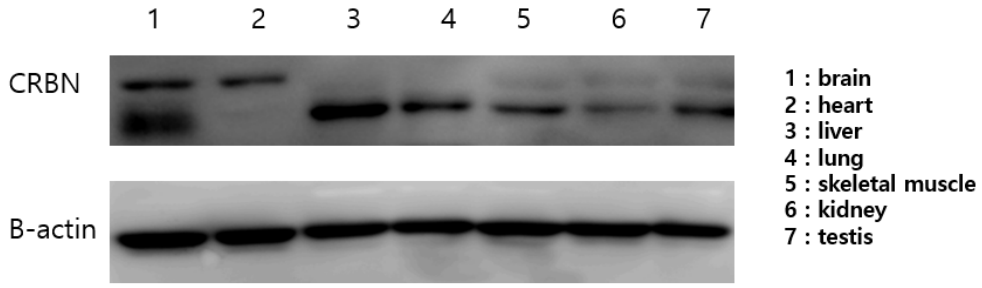

Figure 4. Expression of CRBN in various tissues.

To examine the expression pattern of the CRBN protein in various tissues and validate the bioinformatics results, protein samples were obtained from the Br, brain; H, heart; Li, liver; L, lung; SM, skeletal muscle; K, kidney; T, testis; lysate expressing CRBN. Western blot analysis was conducted using the newly developed antibody. Approximately, 50 μg of tissue proteins was loaded and blotted using mouse anti-CRBN antibody (1:1000)

A.

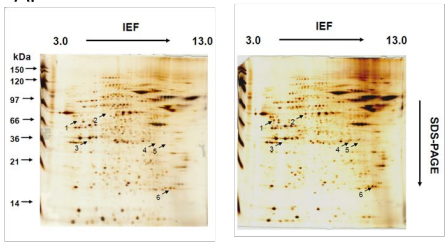

B.

Spot	Identified protein	Accession number	Est. Z	PI/MM
1	Keratin 8, type II cytoskeletal	P05787	2.39	5,52/53,54
2	Heat shock protein 90-kD (hsp90)	P07900	2.13	6,94/84,54
3	β-Actinin (F-actin cross linking protein)	O43707	0.98	6,32/42,85
4	Annexin II (lipocortin II)	P07355	1.62	7,56/38,47
5	Guanine nucleotide-binding protein -I subunit (G(i) 1)	P04898	1.82	8.35/40.91
6	Myosin light chain, non-muscle isoform	P16475	1.83	10.6/17,08

Figure 5. Various proteins included in purified CRBN protein

After purifying CRBN, various proteins can be identified when 2d gel electrophoresis is performed. (a) The type of protein in 6 spots was confirmed. (b)

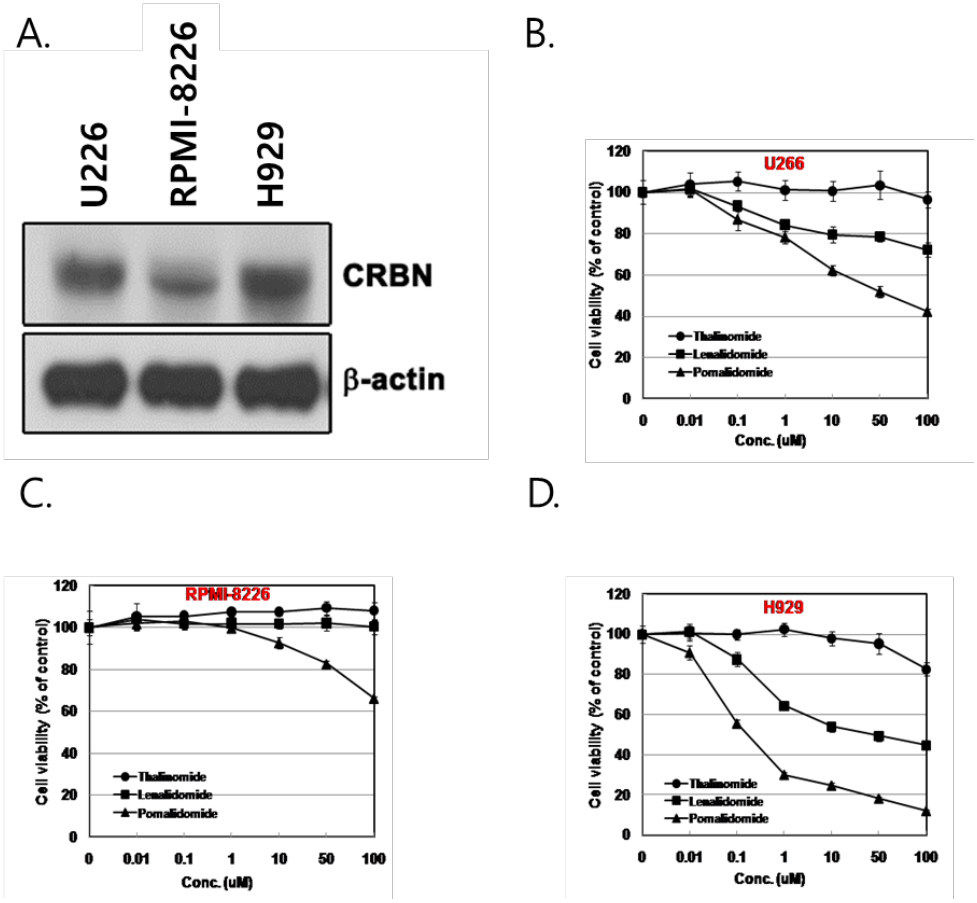

Figure 6. Anti-cancer effect of IMiDs according to CRBN level and level in multiple myeloma cell line.

Levels of CRBN in multiple myeloma cell lines(a) Ant-icancer effect according to type when treated with IMiDs for 24 hours in U226 cells. (b) Anti-cancer effect according to type when treated with IMiDs for 24 hours in RPMI-8226 cells. (c) Anti-cancer effect according to type when treated with IMiDs for 24 hours in H929 cells. (d)

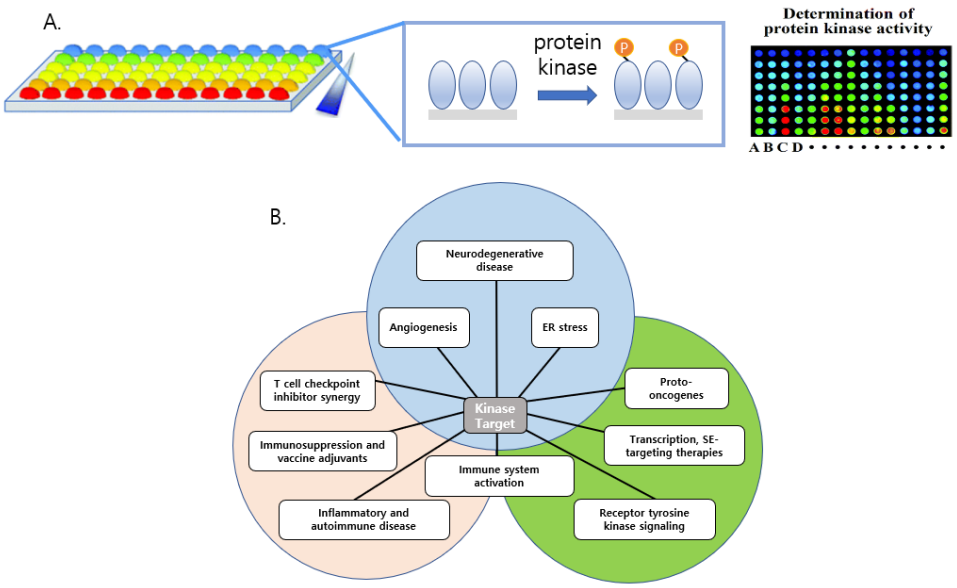

Figure 7. Kinase target binding to CRBN and various biological processes.

Through a Protein Kinase Assay, we investigated proteins interacting with CRBN using an ELISA, obtaining higher absorbance values with increased reactivity. (a) Proteins that exhibited a strong response in the ELISA were further examined for their involvement using bioinformatics to identify associated proteins. (b)

A.

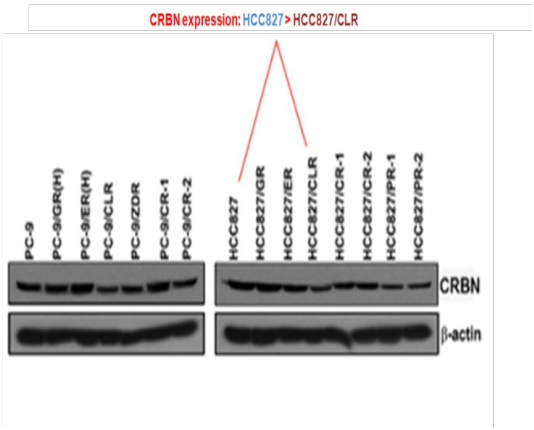

B.

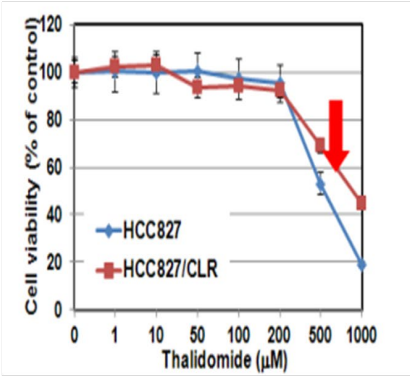

Figure 8. Efficacy of IMiDs in lung cancer.

CRBN levels in Lung cancer cell lines. (a) Comparison of CRBN levels in different Lung cancer cell lines. (b) Anticancer effect of IMiDs in cells with high CRBN protein expression level and cells with low CRBN protein expression level.

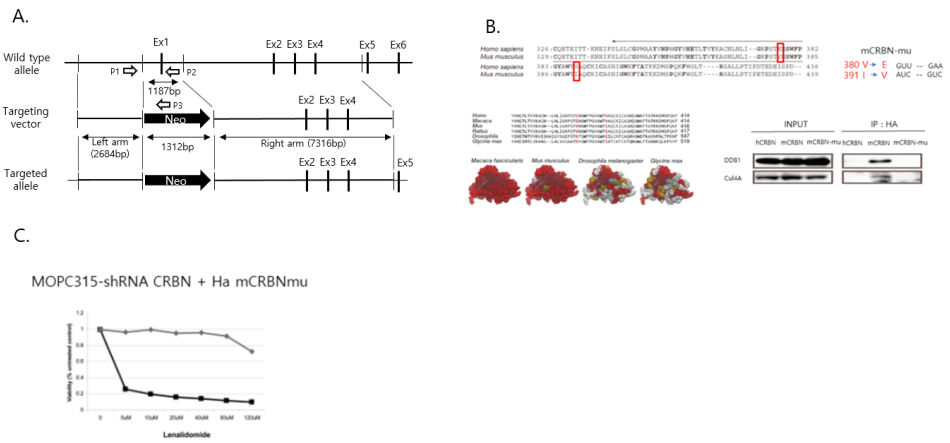

Figure 9. CRBN KO mouse construction and humanization of CRBN.

The vector construct used to generate CRBN KO (CRBN−/−) mice. The genotyping primers are indicated as P1, P2, and P3. (a) Humanized CRBN(b) Anti-cancer effect of IMiDs when MOPC315 cell line is replaced with humanized CRBN(c)

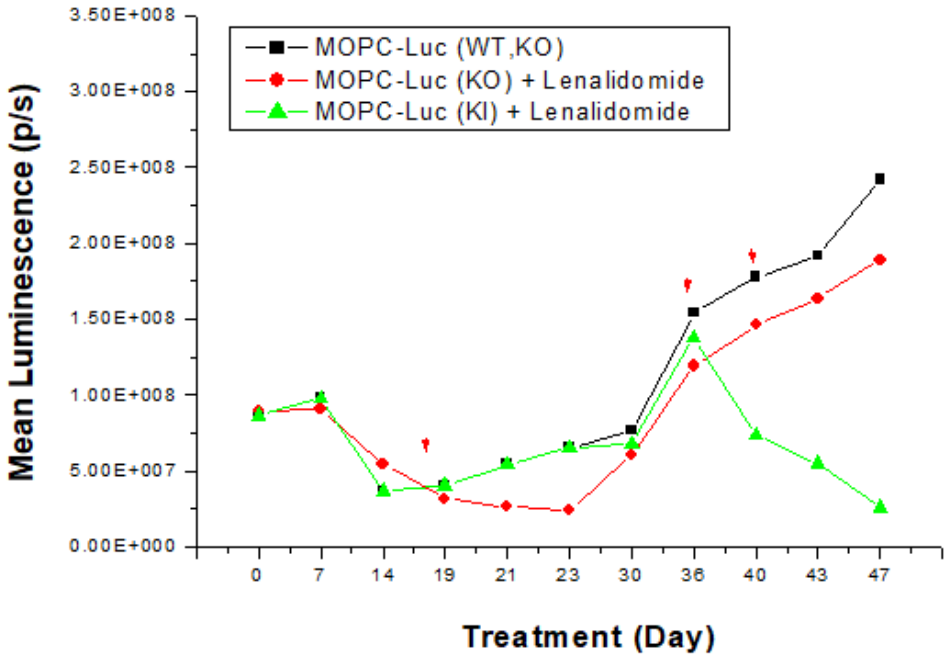

Figure 10. Anti-cancer effects of IMiDs according to CRBN in CDX animal models.

Anti-cancer effects of IMiDs in animal models using MOPC-Luc Cell for 47 days.

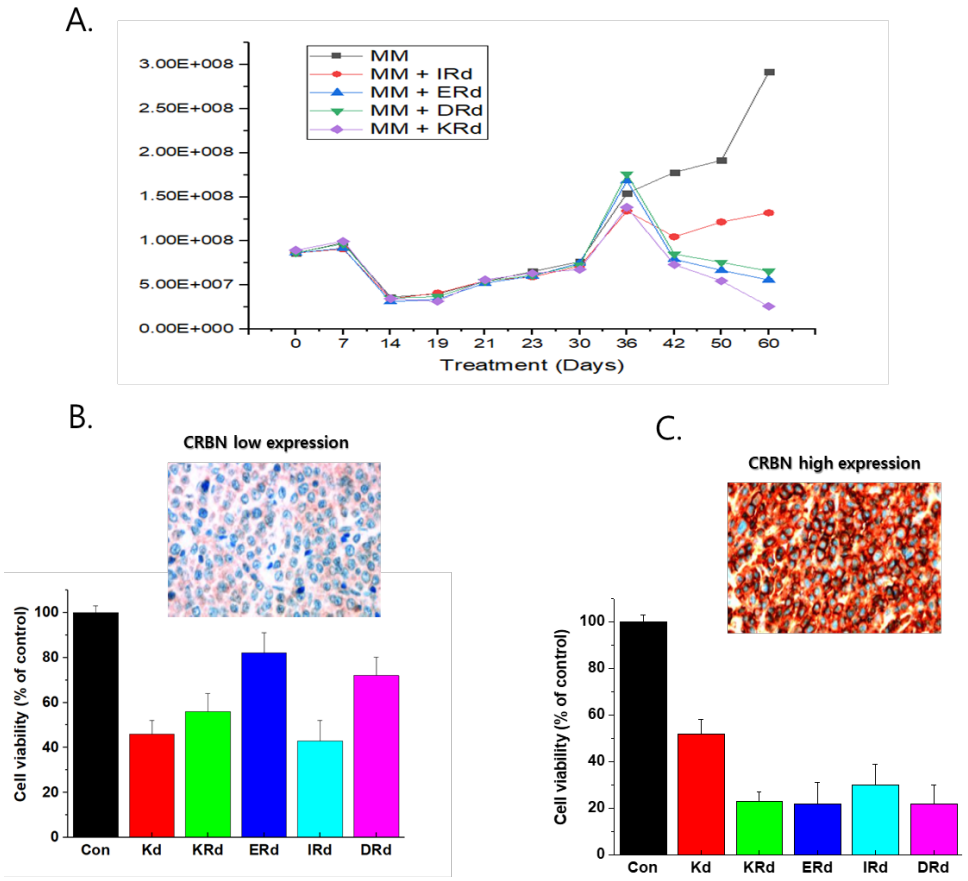

Figure 11. Effectiveness of anticancer drugs according to CRBN level in multiple myeloma animal models.

Treatment effects according to CRBN level and anticancer drug type in multiple myeloma models. (a) Treatment effect according to type of anticancer drug at low CRBN level. (b) Treatment effect according to type of anticancer drug at high CRBN level. (c)

Discussion

In this study, A new CRBN monoclonal antibody was developed using hybridoma cells due to the inadequate performance of previously available and widely used CRBN antibodies. When compared to the existing CRBN antibodies that have been commercially available and utilized, the newly produced CRBN monoclonal antibody demonstrated precise functionality in Western blot analysis and effectively operated in tissue staining assays. Using the newly developed CRBN monoclonal antibody, we investigated the expression levels of CRBN protein in various organs, confirming its expression across different tissues.

The investigation into the expression levels of the CRBN protein revealed its presence in various tissues, including the heart, brain, lungs, liver, skeletal muscles, kidneys, and testes. Among these, the highest expression was observed in the brain and immune cells, as confirmed by Western blot analysis.

The anti-cancer effect of IMiDs according to CRBN expression was measured in Multiple myeloma cell lines (U266, RPMI8226, H929). Among the three cell lines (U266, RPMI8226, H929), H929 cells had the highest CRBN expression, RPMI8226 had the lowest CRBN expression, and U266 showed moderate CRBN expression.

According to the expression of CRBN, H929 cells with the highest CRBN expression were the best, RPMI8226 cells with the lowest CRBN expression were the least affected, and U266 cells also showed moderate results depending on the amount of CRBN expression. As a result, I can say that the anti-cancer effect of IMiDs is related to the amount of CRBN expression.

To investigate the impact of CRBN expression on the anti-cancer effects of IMiDs in cancers other than multiple myeloma, the expression levels of CRBN were examined in lung cancer cells. The results revealed that CRBN expression was higher in HCC827 cells compared to HCC827/CLR cells, and the IMiDs-induced cytotoxicity was consequently increased. This finding suggests that the efficacy of IMiDs in inducing cellular toxicity may be modulated by the level of CRBN

expression not only in multiple myeloma but also in other cancer types.

In addition, CRBN Knockout Mice and Humanized CRBN Knock in Mice were produced to evaluate the effectiveness of CRBN protein-related anti-cancer drugs and to study mechanisms using animal models, and stronger anti-cancer effects were identified in Humanized CRBN Knock in when investigating the IMiDs anti-cancer effects of CRBN Knockout and Humanized CRBN Knock in using MOPC315 cells

Humanized CRBN knock in Mice confirmed cancer cell regeneration and proliferation inhibition by increase of il-2. In addition, Multiple myeloma animal models implanted with MOPC315-Luc cells in CRBN Knockout Mice and Humanized CRBN Knock in Mice were investigated for the anti-cancer effect during lenalidomide treatment, and the dramatic tumor reduction in humanized CRBN knock in Mice was also shown. All these results showed that CRBN directly affected the anti-cancer effect of IMiDs, and the higher the expression of CRBN, the better the anti-cancer effect. Finally, in order to investigate the selection criteria for therapeutic agents according to the expression of CRBN in Multiple myeloma animal models, combination therapy drugs containing IMiDs showed dramatic therapeutic effects in high CRBN expression when combination therapy drugs were treated with low and high expression of CRBN. This means that the higher the patient's CRBN expression after pre-investigation, the better the treatment effect can be expected when combined with IMiDs. In this study, pre-investigation of the expression of CRBN in patients is necessary to establish selection criteria for selective treatment in Multiple myelomas, and we can say that CRBN is an important target for selecting treatments in Multiple myelomas. In addition, In order to confirm the contents of CRBN and IMiDs, knock in mouse and knock out mouse were produced, and the results of using animal models using the produced animals were presented in this paper.

When considering the overall results, it is suggested that the efficacy of IMiDs in the treatment of multiple myeloma (MM) may be influenced by the expression levels of cereblon (CRBN) in the tumor cells. Therefore, it is hypothesized that initiating combination therapy, particularly incorporating IMiDs, may be more effective in MM patients with higher CRBN expression. This proposition implies that

prioritizing the treatment of MM patients with elevated CRBN expression with a combination therapy involving IMiDs could be advantageous.

This information could serve as foundational data suggesting that CRBN in MM may serve as a novel target protein for selecting therapeutic agents.

References

1. Higgins, J.J., et al., Neurology, 2000. **55**(3): p. 335-40. *A gene for nonsyndromic mental retardation maps to chromosome 3p25-pter.*
2. Higgins, J.J., et al., Neurology, 2004. **63**(10): p. 1927-31. *A mutation in a novel ATP-dependent Lon protease gene in a kindred with mild mental retardation.*
3. Shi, Q. and L. Chen, J Immunol Res, 2017. **2017**: p. 9130608. *Cereblon: A Protein Crucial to the Multiple Functions of Immunomodulatory Drugs as well as Cell Metabolism and Disease Generation.*
4. Gandhi, A.K., et al., Br J Haematol, 2014. **164**(2): p. 233-44. *Measuring cereblon as a biomarker of response or resistance to lenalidomide and pomalidomide requires use of standardized reagents and understanding of gene complexity.*
5. Jackson, S. and Y. Xiong, Trends Biochem Sci, 2009. **34**(11): p. 562-70. *CRL4s: the CUL4-RING E3 ubiquitin ligases.*
6. Cheng, J., et al., Biochim Biophys Acta Rev Cancer, 2019. **1871**(1): p. 138-159. *The emerging role for Cullin 4 family of E3 ligases in tumorigenesis.*
7. Jo, S., et al., J Neurochem, 2005. **94**(5): p. 1212-24. *Identification and functional characterization of cereblon as a binding protein for large-conductance calcium-activated potassium channel in rat brain.*
8. Moon, H., et al., Nat Commun, 2020. **11**(1): p. 5489. *CRBN modulates calcium influx by regulating Orai1 during efferocytosis.*
9. Yang, S.J., et al., Pharmaceuticals (Basel), 2021. **14**(6). *Regulation of AMPK Activity by CRBN Is Independent of the Thalidomide-CRL4(CRBN) Protein Degradation Axis.*
10. Lee, K.M., et al., Biochim Biophys Acta, 2011. **1813**(3): p. 448-55. *Functional modulation of AMP-activated protein kinase by cereblon.*
11. Min, Y., et al., Cell Death Dis, 2016. **7**(7): p. e2313. *Cereblon negatively regulates TLR4 signaling through the attenuation of ubiquitination of TRAF6.*
12. Kim, M.J., et al., Front Immunol, 2019. **10**: p. 2203. *CRBN Is a Negative Regulator of Bactericidal Activity and Autophagy Activation Through Inhibiting the Ubiquitination of ECSIT and BECN1.*

13. Yang, J., et al., J Biol Chem, 2018. **293**(26): p. 10141-10157. *Cereblon suppresses the lipopolysaccharide-induced inflammatory response by promoting the ubiquitination and degradation of c-Jun.*
14. Kang, J.A., et al., Proc Natl Acad Sci U S A, 2016. **113**(31): p. 8771-6. *Epigenetic regulation of Kcna3-encoding Kv1.3 potassium channel by cereblon contributes to regulation of CD4+ T-cell activation.*
15. Lee, K.M., et al., Biochem Biophys Res Commun, 2015. **458**(1): p. 34-9. *Depletion of the cereblon gene activates the unfolded protein response and protects cells from ER stress-induced cell death.*
16. Akber, U., et al., J Neurosci, 2021. **41**(24): p. 5138-5156. *Cereblon Regulates the Proteotoxicity of Tau by Tuning the Chaperone Activity of DNAJA1.*
17. Kim, J., et al., Biochem Biophys Res Commun, 2014. **447**(4): p. 649-54. *Ablation of cereblon attenuates myocardial ischemia-reperfusion injury.*
18. Park, N., et al., Eur Heart J, 2022. **43**(20): p. 1973-1989. *Cereblon contributes to cardiac dysfunction by degrading Cav1.2alpha.*
19. Lee, K.M., et al., Diabetes, 2013. **62**(6): p. 1855-64. *Disruption of the cereblon gene enhances hepatic AMPK activity and prevents high-fat diet-induced obesity and insulin resistance in mice.*
20. Kim, Y.D., et al., Biochim Biophys Acta, 2015. **1852**(12): p. 2662-70. *Inhibition of cereblon by fenofibrate ameliorates alcoholic liver disease by enhancing AMPK.*
21. An, S., et al., Exp Mol Med, 2023. **55**(7): p. 1556-1569. *Enhancement of the SESN2-SHP cascade by melatonin ameliorates hepatic gluconeogenesis by inhibiting the CRBN-BTG2-CREBH signaling pathway.*
22. Lee, S.E., et al., J Pineal Res, 2020. **68**(3): p. e12638. *Induction of SIRT1 by melatonin improves alcohol-mediated oxidative liver injury by disrupting the CRBN-YY1-CYP2E1 signaling pathway.*
23. Gil, M., et al., Biochem Biophys Res Commun, 2018. **495**(1): p. 976-981. *Cereblon deficiency confers resistance against polymicrobial sepsis by the activation of AMP activated protein kinase and heme-oxygenase-1.*
24. Yao, C., et al., Biochem Biophys Res Commun, 2018. **496**(3): p. 967-974. *Cereblon (CRBN) deletion reverses streptozotocin induced diabetic osteoporosis in mice.*
25. Jeon, S., et al., Aging (Albany NY), 2021. **13**(5): p. 6406-6419. *Ablation of*

CRBN induces loss of type I collagen and SCH in mouse skin by fibroblast senescence via the p38 MAPK pathway.

26. Yamamoto, J., et al., Chem Soc Rev, 2022. **51**(15): p. 6234-6250. *Discovery of CRBN as a target of thalidomide: a breakthrough for progress in the development of protein degraders.*
27. Gao, S., et al., Biomed Pharmacother, 2020. **127**: p. 110114. *Recent advances in the molecular mechanism of thalidomide teratogenicity.*
28. Ito, T. and H. Handa, Int J Hematol, 2016. **104**(3): p. 293-9. *Cereblon and its downstream substrates as molecular targets of immunomodulatory drugs.*
29. Chang, X., et al., Acta Biochim Biophys Sin (Shanghai), 2014. **46**(3): p. 240-53. *Mechanism of immunomodulatory drugs' action in the treatment of multiple myeloma.*
30. Sheskin, J., Clin Pharmacol Ther, 1965. **6**: p. 303-6. *Thalidomide in the Treatment of Lepra Reactions.*
31. Okafor, M.C., Pharmacotherapy, 2003. **23**(4): p. 481-93. *Thalidomide for erythema nodosum leprosum and other applications.*
32. Faver, I.R., et al., Int J Dermatol, 2005. **44**(1): p. 61-7. *Thalidomide for dermatology: a review of clinical uses and adverse effects.*
33. Ito, T., et al., Science, 2010. **327**(5971): p. 1345-50. *Identification of a primary target of thalidomide teratogenicity.*
34. D'Amato, R.J., et al., Proc Natl Acad Sci U S A, 1994. **91**(9): p. 4082-5. *Thalidomide is an inhibitor of angiogenesis.*
35. Bramuzzo, M., et al., Medicine (Baltimore), 2016. **95**(30): p. e4239. *Thalidomide for inflammatory bowel disease: Systematic review.*
36. Chasset, F., et al., J Am Acad Dermatol, 2018. **78**(2): p. 342-350 e4. *Efficacy and tolerance profile of thalidomide in cutaneous lupus erythematosus: A systematic review and meta-analysis.*
37. Raje, N. and K. Anderson, N Engl J Med, 1999. **341**(21): p. 1606-9. *Thalidomide--a revival story.*
38. Rajkumar, S.V., et al., Leukemia, 2001. **15**(8): p. 1274-6. *Thalidomide for previously untreated indolent or smoldering multiple myeloma.*
39. Kumar, S. and S.V. Rajkumar, Expert Rev Anticancer Ther, 2005. **5**(5): p. 759-66. *Thalidomide and dexamethasone: therapy for multiple myeloma.*
40. Kim, B.S., et al., Transplant Proc, 2015. **47**(3): p. 787-90. *Immune*

modulatory effect of thalidomide on T cells.

41. Majumdar, S., B. Lamothe, and B.B. Aggarwal, J Immunol, 2002. **168**(6): p. 2644-51. *Thalidomide suppresses NF-kappa B activation induced by TNF and H2O2, but not that activated by ceramide, lipopolysaccharides, or phorbol ester.*
42. Franks, M.E., G.R. Macpherson, and W.D. Figg, Lancet, 2004. **363**(9423): p. 1802-11. *Thalidomide.*
43. Vallet, S., et al., Leuk Lymphoma, 2008. **49**(7): p. 1238-45. *Thalidomide and lenalidomide: Mechanism-based potential drug combinations.*
44. Lee, S.W., et al., Rheumatology (Oxford), 2012. **51**(12): p. 2131-40. *Attenuation of nephritis in lupus-prone mice by thalidomide.*
45. Tseng, C.M., et al., Lung, 2013. **191**(4): p. 361-8. *The suppression effects of thalidomide on human lung fibroblasts: cell proliferation, vascular endothelial growth factor release, and collagen production.*
46. Yndestad, A., et al., Eur J Heart Fail, 2006. **8**(8): p. 790-6. *Thalidomide attenuates the development of fibrosis during post-infarction myocardial remodelling in rats.*
47. Kim, D.H., et al., Eur J Heart Fail, 2010. **12**(10): p. 1051-60. *The protective effect of thalidomide on left ventricular function in a rat model of diabetic cardiomyopathy.*
48. Lv, P., et al., Mediators Inflamm, 2006. **2006**(4): p. 93253. *Effects of thalidomide on the expression of adhesion molecules in rat liver cirrhosis.*
49. Di Raimondo, F., et al., Haematologica, 2000. **85**(8): p. 800-5. *Angiogenic factors in multiple myeloma: higher levels in bone marrow than in peripheral blood.*
50. Rajkumar, S.V., et al., Leukemia, 1999. **13**(3): p. 469-72. *Bone marrow angiogenesis in patients achieving complete response after stem cell transplantation for multiple myeloma.*
51. Barlogie, B., et al., N Engl J Med, 2006. **354**(10): p. 1021-30. *Thalidomide and hematopoietic-cell transplantation for multiple myeloma.*
52. Zhou, L., et al., BMC Cancer, 2021. **21**(1): p. 606. *Measuring the global, regional, and national burden of multiple myeloma from 1990 to 2019.*
53. Nijhof, I.S., et al., Drugs, 2018. **78**(1): p. 19-37. *Current and New Therapeutic Strategies for Relapsed and Refractory Multiple Myeloma: An Update.*

54. Lu, G., et al., Science, 2014. **343**(6168): p. 305-9. *The myeloma drug lenalidomide promotes the cereblon-dependent destruction of Ikaros proteins.*
55. Kortum, K.M., et al., Blood Rev, 2015. **29**(5): p. 329-34. *Cereblon binding molecules in multiple myeloma.*
56. Kronke, J., et al., Science, 2014. **343**(6168): p. 301-5. *Lenalidomide causes selective degradation of IKZF1 and IKZF3 in multiple myeloma cells.*
57. Gandhi, A.K., et al., Br J Haematol, 2014. **164**(6): p. 811-21. *Immunomodulatory agents lenalidomide and pomalidomide co-stimulate T cells by inducing degradation of T cell repressors Ikaros and Aiolos via modulation of the E3 ubiquitin ligase complex CRL4(CRBN.).*
58. Lopez-Girona, A., et al., Leukemia, 2012. **26**(11): p. 2326-35. *Cereblon is a direct protein target for immunomodulatory and antiproliferative activities of lenalidomide and pomalidomide.*

국문요약

다발성 골수종(Multiple myloma, MM)의 치료는 효과성 때문에 병용 요법을 우선시하지만, 그 중 MM 의 대표적인 항암제로 면역조절 약물(IMiDs, Immune modulating drug)들이 주로 사용되고 있으며, 그 작용기전으로 IMiDs 는 E3 ubiquitin ligase complex 의 subunit 인 CRBN 단백에 결합하여 그 기질을 변경시킴으로써, 특정 단백질 Ikaros (IKZF1) 와 Aiolos (IKZF3)의 유비퀴틴화를 유도하여 세포 사멸을 유도하거나 세포 주기를 조절하여 종양의 성장을 억제하는 방식으로 이루어집니다.

CRBN 단백의 발현을 조사하기 위해 특이적으로 CRBN 에 결합하는 단일클론 항체를 하이브리도마 세포를 이용하여 제작하였고, 여러 조직에서의 CRBN 단백발현 수준을 조사한 결과 CRBN 단백의 발현은 심장, 뇌, 폐, 간, 골격근, 신장 및 고환을 포함한 다양한 조직에서 확인할 수 있었습니다. 그 중 가장 많이 발현되는 부분으로 뇌, 면역세포 등에서 많이 발현되는 것을 western blot 을 이용해 확인하였습니다. 더 나아가 CRBN 단백의 기능을 확인하기 위하여 CRBN knock out mice 를 제작하였으며, 이를 활용하여 정상 생쥐와 KO 생쥐의 뇌조직을 이용하여 CRBN 과 연관된 단백을 조사하기 위해 2D 전기영동을 사용하여 발현의 차이가 있는 단백을 분리하고 분석을 통해 5 개의 발현 차이가 나는 단백을 찾았으며, 또한 이러한 샘플을 활용하여 protenn kinase assay 방법을 통하여 CRBN 단백 관련 메커니즘을 조사한 결과 기존 문헌에 나온 것처럼 CRBN 단백이 E3 ubiquitin ligase pathway 와 연관성이 있음을 확인하였습니다.

위 결과들을 종합하여 다발성 골수종 세포주에서 CRBN 단백 발현과 IMD 의 세포독성을 조사하였습니다. MM 인간 세포주들 (U226, RPMI-8226, H929)에서의 CRBN 발현을 조사한 결과 RPMI-8226, U226 H929 순으로

발현율이 높은 것을 확인하였으며, CRBN 발현이 높을수록 IMiDs 세포독성 효능이 증가하는 것을 발견하였습니다.

추가적으로 다른 암 종인 폐암의 세포에서도 HCC827/CLR 세포에 비해 HCC827 세포에서 CRBN 발현이 더 높고 IMiDs 세포독성 효능 또한 다발성 골수종 세포주와 동일하게 증가한 것을 조사하였습니다. 이러한 결과를 종합해 볼 때 다발성 골수종인 뿐만 아니라 CRBN 발현이 증가되어 있는 폐암세포주에서도 CRBN 발현이 낮은 폐암세포주에 비해 CRBN 발현이 높은 폐암세포주에서 IMDs 가 세포독성 효능이 증가한다고 말씀드릴 수 있습니다.

기존 보고에서 알려진 대로 IMDs 의 세포독성의 효능은 설치류에서는 거의 나타나지 않았고, 인간의 경우에서만 나타난다는 보고를 참조하여 아미노산 2 개를 변형시킨 humanized CRBN 녹인(KI) 마우스를 제작하였습니다. 이러한 CRBN KI 동물모델을 이용하여 생쥐의 다발성 골수종 세포주인 MOPC315-Luc (humanized CRBN)세포주를 활용하여 다발성 골수종 동물모델을 구축하였습니다. 이러한 모델을 활용하여 조사한 결과 CRBN KO 및 KI 두 동물모델에 MOPC315-Luc 세포주를 이식한 후에 47 일 동안 IMDs 를 처리하였을 때 CRBN KO 마우스에 비해 humanized CRBN KI 마우스에서 다발성 골수종의 크기가 유의성 있게 감소하였습니다.

이러한 결과들을 종합해 볼 때 MM 에서 치료 시 CRBN 단백 발현 정도가 IMiDs 의 효능에 영향을 주기 때문에 높은 CRBN 의 발현이 높은 MM 환자에게 먼저 IMiDs 가 포함된 병용요법을 우선 치료하는 것이 효과적일 것이라 사료됩니다.

이는 MM 에서 CRBN 은 치료제를 선별하기 위한 새로운 표적 단백으로 사용될 수 있는 기초자료로 활용될 수 있을 것입니다.

핵심주제어: 다발성 골수종, 세레블론, 면역조절제